The following Communications have been judged by at least two referees to be "very important papers" and will be published online at www.angewandte.org soon:

*T. Lewis, M. Faubel, B. Winter, J. C. Hemminger**
CO_2 Capture in an Aqueous Solution of an Amine: Role of the Solution Interface

*Y. H. Kim, S. Banta**
Complete Oxidation of Methanol in an Enzymatic Biofuel Cell by a Self-Assembling Hydrogel Created from Three Modified Dehydrogenases

*W. Gan, B. Xu, H.-L. Dai**
Activation of Reactions of Thiols at the Silver-Nanoparticle Surface

*M. Sasaki, Y. Kondo, M. Kawahata, K. Yamaguchi, K. Takeda**
Enantioselective Synthesis of Siloxyallenes from Alkynoyl Silanes by Reduction and a Brook Rearrangement and Their Subsequent Trapping in a [4+2] Cycloaddition with Unusual Facial Selectivity

H. S. Choi, K. Nasr, S. Alyabyev, D. Feith, J. H. Lee, S. H. Kim, Y. Ashitate, H. Hyun, G. Patonay, L. Strekowski, M. Henary, J. V. Frangioni**
Zwitterionic Near-Infrared Fluorophores and Their Fate In Vivo

A. Bonet, C. Pubill-Ulldemolins, C. Bo, H. Gulyás,* E. Fernández**
Transition-Metal-Free Diboration by the Activation of Diboron Compounds with Simple Lewis Bases

M. Evangelisti, O. Roubeau, E. Palacios, A. Camón, T. N. Hooper, E. K. Brechin, J. J. Alonso*
Cryogenic Magnetocaloric Effect in a Ferromagnetic Molecular Dimer

*W. Liu, V. Khedkar, B. Baskar, M. Schürmann, K. Kumar**
Branching Cascades: A Concise Synthetic Strategy Targeting Diverse and Complex Molecular Frameworks

Author Profile

"The biggest problem that scientists face is the efficient utilization of solar energy.
If I won the lottery, I would buy as many sports cars of all kinds as possible …"
This and more about Kenichiro Itami can be found on page 5794.

Books

Highlights

Two functions are important: Three examples of well-defined bifunctional iron catalysts that are very efficient in the hydrogenation of ketones are described (see scheme). These remarkable studies will contribute significantly to the development of more environmentally friendly and sustainable reduction reactions in the near future.

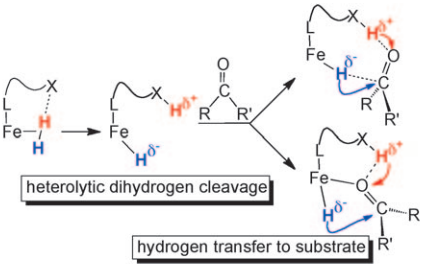

Iron Catalysis

New targets, new drugs: In the context of regulating gene expression, small molecules have been found that specifically disrupt the interaction between the "reader" (e.g. a protein with a bromodomain) and chromatin. These results provide compelling proof-of-concept that disrupting histone readers is a viable strategy for the development of epigenetic drugs. (The picture shows the complex formed by (+)-JQ1 and the bromodomain hBRD2.)

Worth one's while: The careful use of a single chromophore on methodically designed polymers can be sufficient to modify polymer properties. Recent examples range from controlled micelle destruction and light-controlled precipitation in aqueous solution to the fabrication of nanoporous thin films (see schematic illustration of the use of a photocleavable block copolymer as a template for a nanoporous thin film).

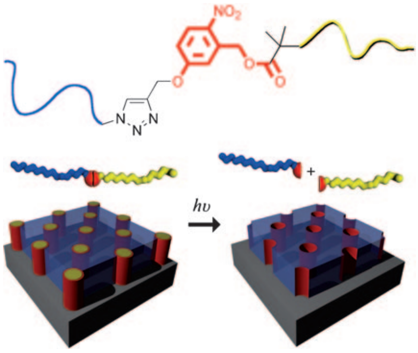

Reviews

Long becomes short: During upconversion (UC), absorption of several long-wavelength photons leads to emission of short-wavelength radiation. Current methods allow the synthesis of highly efficient, small UC particles with narrow size distribution able to form transparent solutions in a wide range of solvents (see photo of UC luminescence in nanocrystal solutions), and new synthetic routes are available to tune important properties of UC nanocrystals.

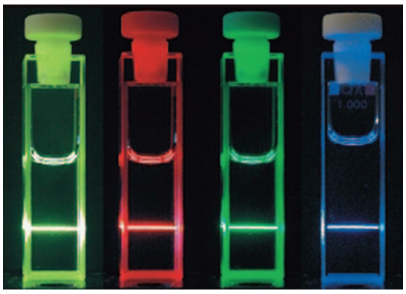

For the USA and Canada:
ANGEWANDTE CHEMIE International Edition (ISSN 1433-7851) is published weekly by Wiley-VCH, PO Box 191161, 69451 Weinheim, Germany. Air freight and mailing in the USA by Publications Expediting Inc., 200 Meacham Ave., Elmont, NY 11003. Periodicals postage paid at Jamaica, NY 11431. US POSTMASTER: send address changes to *Angewandte Chemie*, Journal Customer Services, John Wiley & Sons Inc., 350 Main St., Malden, MA 02148-5020. Annual subscription price for institutions: US$ 9442/8583 (valid for print and electronic / print or electronic delivery); for individuals who are personal members of a national chemical society prices are available on request. Postage and handling charges included. All prices are subject to local VAT/ sales tax.

Hydrogenation

I. Nakamula, Y. Yamanoi, T. Imaoka,
K. Yamamoto,*
H. Nishihara* ________ 5830–5833

A Uniform Bimetallic Rhodium/Iron Nanoparticle Catalyst for the Hydrogenation of Olefins and Nitroarenes

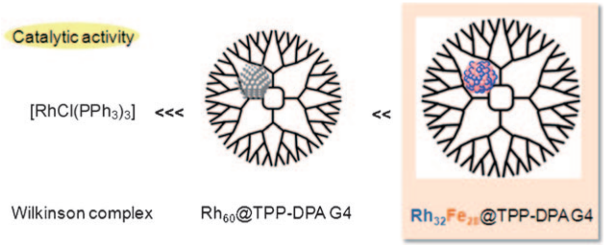

Mix and more than match: Relative to the catalytic activity of pure Rh nanoparticles in a dendrimer cage, Rh/Fe bimetallic nanoparticles in dendrimers have improved catalytic activity towards the hydrogenation of olefins, and unlike Wilkinson catalyst could catalyze nitroarene hydrogenation (see scheme, G4 = 4th generation dendrimer).

Asymmetric Catalysis

A. Rudolph, P. H. Bos, A. Meetsma,
A. J. Minnaard,
B. L. Feringa* ________ 5834–5838

Catalytic Asymmetric Conjugate Addition/Oxidative Dearomatization Towards Multifunctional Spirocyclic Compounds

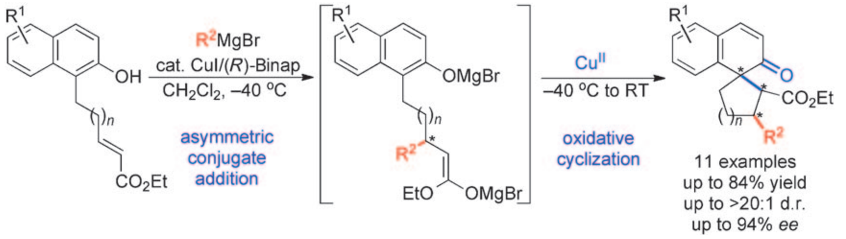

Naphthol compounds bearing a pendant α,β-unsaturated ester undergo a copper(I)-catalyzed asymmetric conjugate addition/copper(II)-mediated intramolecular oxidative coupling to afford benzo-fused spirocyclic cyclohexenones (see scheme). This one-pot strategy results in two new carbon–carbon bonds and three contiguous stereocenters. The products contain a high degree of functionality and molecular complexity.

Metabolic Exchange

Y.-L. Yang, Y. Xu, R. D. Kersten, W.-T. Liu,
M. J. Meehan, B. S. Moore, N. Bandeira,
P. C. Dorrestein* ________ 5839–5842

Connecting Chemotypes and Phenotypes of Cultured Marine Microbial Assemblages by Imaging Mass Spectrometry

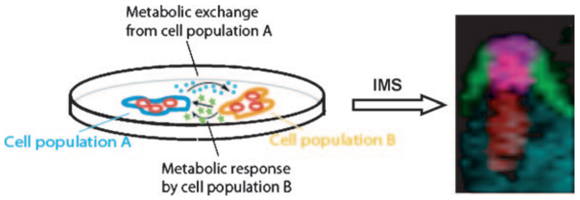

Deciphering the language of bacteria: Imaging mass spectrometry (IMS) of a marine environmental sample revealed that a secreted peptide from an immobile *Promicromonosporaceae* strain alters the mobility of a motile *Bacillus subtilis* strain. The *Promicromonosporaceae* also respond to *B. subtilis* by producing hydroxamate siderophores. Thus, multifaceted and multifunctional metabolic exchange between microbes can be captured by IMS (see picture).

Peptide Structures

L. Guo, W. Zhang, A. G. Reidenbach, M. W. Giuliano, I. A. Guzei, L. C. Spencer, S. H. Gellman* ______ **5843 – 5846**

Characteristic Structural Parameters for the γ-Peptide 14-Helix: Importance of Subunit Preorganization

All wound up: Crystallographic data for a set of homologous peptides constructed from gabapentin and two to six preorganized γ-amino acid residues (see crystal structure of the longest peptide) allow derivation of characteristic parameters for the γ-peptide 14-helix and establish guidelines for characterizing 14-helical folding. The results suggest that the substitution pattern of a γ-residue has a profound effect on the propensity for 14-helical folding.

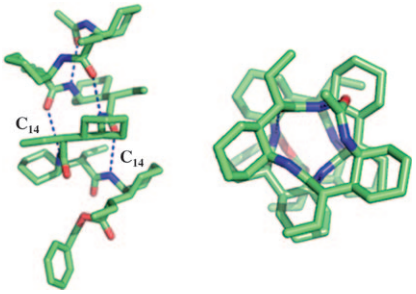

Multiferroics

A. Stroppa,* P. Jain,* P. Barone, M. Marsman, J. M. Perez-Mato, A. K. Cheetham, H. W. Kroto, S. Picozzi ______ **5847 – 5850**

Electric Control of Magnetization and Interplay between Orbital Ordering and Ferroelectricity in a Multiferroic Metal–Organic Framework

Forget me not: In a new multiferroic metal–organic framework (see structure, Cu green, O red, C black, N blue, H gray; arrows show spin configuration), Jahn–Teller and antiferro-distortions induce a switchable ferroelectric polarization, which is coupled to a weak ferromagnetic component. This true magnetoelectric multiferroic should be very attractive for advanced memory devices.

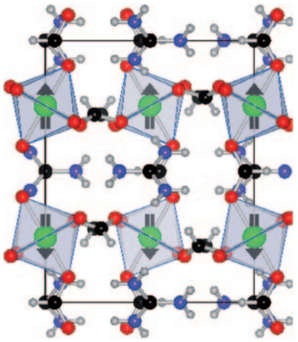

Heterobimetallic Block Copolymers

J. B. Gilroy, S. K. Patra, J. M. Mitchels, M. A. Winnik,* I. Manners* **5851 – 5855**

Main-Chain Heterobimetallic Block Copolymers: Synthesis and Self-Assembly of Polyferrocenylsilane-*b*-Poly(cobaltoceniummethylene)

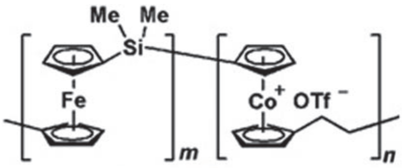

Two metals are better than one: Main-chain heterometallic block copolymers composed of iron- and cobalt-rich blocks (see picture) were synthesized through consecutive photocontrolled ring-opening polymerization (ROP) of sila[1]ferrocenophanes and dicarba[2]cobaltocenophanes followed by oxidation of the cobaltocene-containing block. The redox properties and self-assembly of the resulting block copolymers in solution were also studied.

Self-Organized Hybrid Materials

T. Sakamoto, Y. Nishimura, T. Nishimura, T. Kato* ______ **5856 – 5859**

Photoimaging of Self-Organized $CaCO_3$/Polymer Hybrid Films by Formation of Regular Relief and Flat Surface Morphologies

Picture this! A photoimage written in a reactive polymer with UV light is transferred into $CaCO_3$ crystal morphologies (see picture). The $CaCO_3$ crystal films with microscopic regular relief structures and flat surfaces are self-organized on the nonirradiated and UV-irradiated areas of the polymer matrix, respectively.

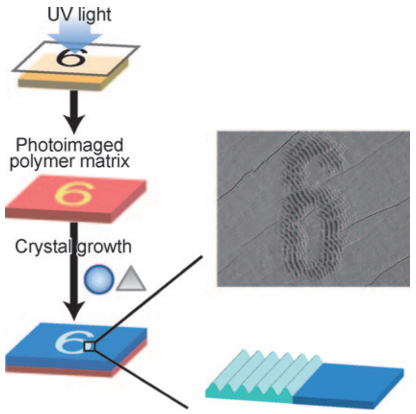

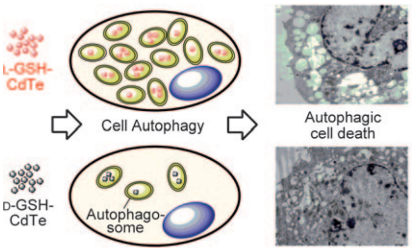

Choose your poison: Chiral CdTe quantum dots (QDs) coated with L- or D-glutathione (GSH) stabilizers exhibit differences in cytotoxicity although they have identical composition and size. D-GSH-QDs are less cytotoxic than L-GSH-QDs. The ability of QDs to induce cell death is correlated with their ability to induce autophagy, which is chirality-dependent (see picture).

Quantum Dots

Y. Li, Y. Zhou, H. Y. Wang, S. Perrett, Y. Zhao,* Z. Tang,* G. Nie* **5860 – 5864**

Chirality of Glutathione Surface Coating Affects the Cytotoxicity of Quantum Dots

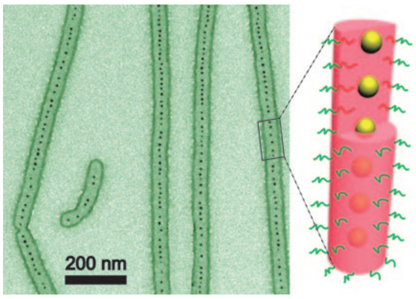

Worm holes: Cylindrical or wormlike block copolymer micelles with gold nanoparticles encapsulated in a micellar core were fabricated through directed supramolecular assembly. This versatile approach allows fine-tuning of interparticle spacing and micellar morphology by varying the content of the nanoparticles or hydrogen bonding agent in the supramolecular assemblies.

Nanostructures

W. K. Li, S. Q. Liu, R. H. Deng, J. T. Zhu* **5865 – 5868**

Encapsulation of Nanoparticles in Block Copolymer Micellar Aggregates by Directed Supramolecular Assembly

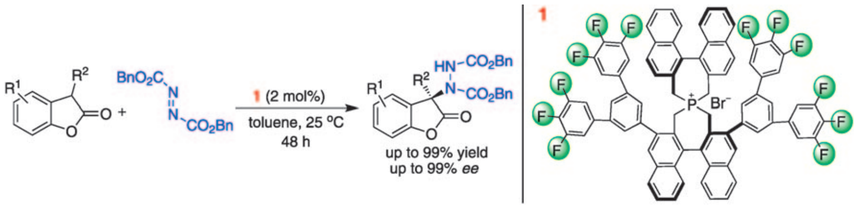

A *spiro*ing reactivity: A series of novel binol-derived *P*-spiro quaternary phosphonium salts were designed, prepared, and used for the first highly enantioselective amination of benzofuranones (see scheme; binol = 1,1′-2-binaphthol, Bn = benzyl). An unprecedented mechanism involving the π–π interactions between the substrate and the catalyst was proposed as the primary binding mode on the basis of molecular modelling and DFT calculations.

Asymmetric Synthesis

C.-L. Zhu, F.-G. Zhang, W. Meng, J. Nie, D. Cahard, J.-A. Ma* **5869 – 5872**

Enantioselective Base-Free Electrophilic Amination of Benzofuran-2(3*H*)-ones: Catalysis by Binol-Derived *P*-Spiro Quaternary Phosphonium Salts

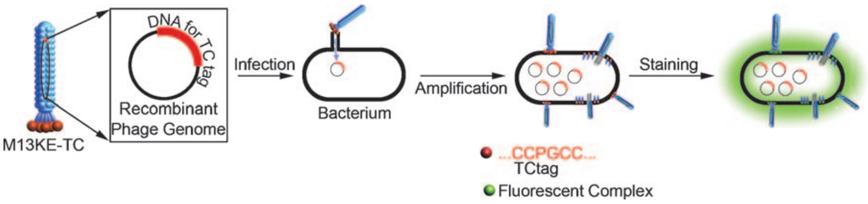

A host-specific phage is genetically modified to tag a tetracysteine (TC) residue to its capsid protein. Upon bacterial infection, the TC tag is expressed on the surface of progeny virions and stained by membrane-permeant biarsenical dye, which results in fluorescence enhancement (see picture). The labeled bacteria are detectable by flow cytometry and fluorescence microscopy.

Bacterial Detection

L. Wu, T. Huang, L. Yang, J. Pan, S. Zhu, X. Yan* **5873 – 5877**

Sensitive and Selective Bacterial Detection Using Tetracysteine-Tagged Phages in Conjunction with Biarsenical Dye

Synthetic Methods

V. Ganesh, D. Sureshkumar,
S. Chandrasekaran* ________ **5878 – 5881**

Tandem Ring Opening/Cyclization of Vinylcyclopropanes: A Facile Synthesis of Chiral Bicyclic Amidines

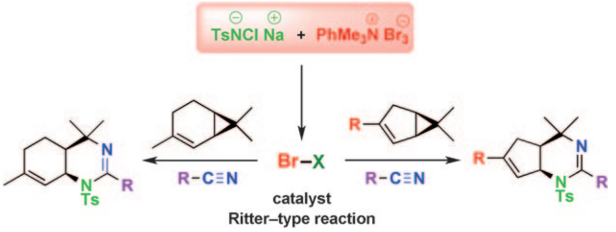

An open and shut case: An interesting bromine-catalyzed tandem ring opening/cyclization reaction of bicyclic vinylcyclopropanes with chloramine-T ([TsNCl]Na) has been demonstrated to furnish chiral bicyclic amidine derivatives in good yield. A plausible mechanism has been proposed based on the experimental observations. Ts = *p*-toluenesulfonyl.

Huge Polymer Circles

Y. Xia, A. J. Boydston,
R. H. Grubbs* ____________ **5882 – 5885**

Synthesis and Direct Imaging of Ultrahigh Molecular Weight Cyclic Brush Polymers

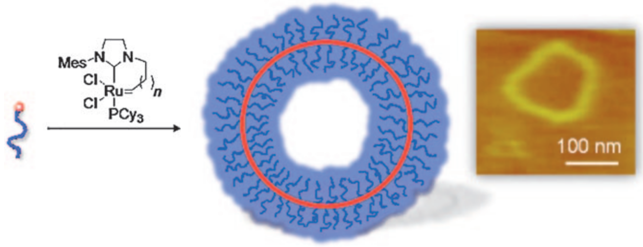

Convenient route to cyclic polymers: Ultrahigh molecular weight cyclic brush polymers were synthesized through ring-expansion metathesis polymerization of various macromonomers. Atomic force microscopy was used to visualize toroidal shapes and large opening pores, along with linear chains, which may result from high sensitivity of brush polymers to mechanical degradation.

Hypergolicity

S. Schneider,* T. Hawkins, Y. Ahmed,
M. Rosander, L. Hudgens,
J. Mills ____________________ **5886 – 5888**

Green Bipropellants: Hydrogen-Rich Ionic Liquids that Are Hypergolic with Hydrogen Peroxide

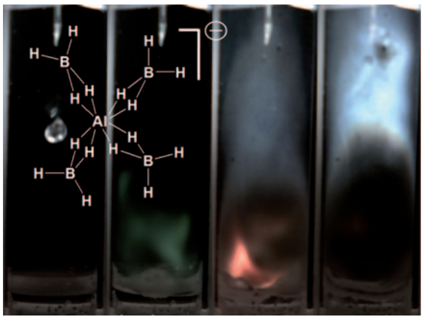

Lift-off: The low vapor toxicity of ionic liquids (ILs) make them attractive replacements for hydrazine in rocket fuel. However, ILs will fail to fulfill their revolutionary promise unless toxic oxidizers such as HNO_3 or N_2O_4 can be replaced with safer alternatives such as H_2O_2. The ILs presented here are hypergolic with H_2O_2 (see picture) and are hydrogen-rich, thus helping to boost performance.

Antibiotics

E. K. Schmitt,* M. Riwanto,
V. Sambandamurthy, S. Roggo, C. Miault,
C. Zwingelstein, P. Krastel, C. Noble,
D. Beer, S. P. S. Rao, M. Au,
P. Niyomrattanakit, V. Lim, J. Zheng,
D. Jeffery, K. Pethe,
L. R. Camacho* ________ **5889 – 5891**

The Natural Product Cyclomarin Kills Mycobacterium Tuberculosis by Targeting the ClpC1 Subunit of the Caseinolytic Protease

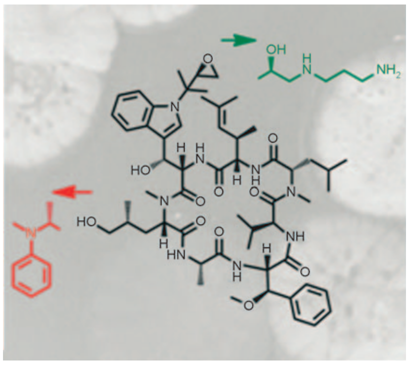

Target practice: The target of the antibiotic cyclomarin A was identified in *Mycobacterium*. Cyclomarin A (see structure) binds the regulatory subunit of the Clp protease complex with high affinity resulting in elevated proteolysis and cell death. The property of cyclomarin to kill both growing and nonreplicating mycobacteria makes the Clp protease a promising target for antitubercular drug discovery.

Natural Product Synthesis

J. M. Tenenbaum, W. J. Morris,
D. W. Custar, K. A. Scheidt* **5892 – 5895**

Synthesis of (−)-Okilactomycin by a Prins-Type Fragment-Assembly Strategy

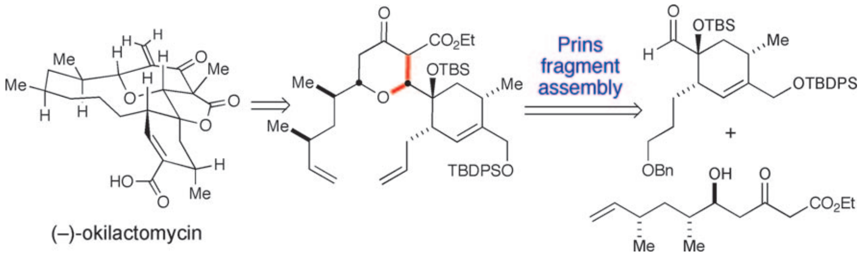

All things converge: A highly convergent synthesis of (−)-okilactomycin utilizes a Prins-type Maitland–Japp cyclization for the fragment assembly of two complex intermediates (see scheme). The synthesis also employs a highly diastereoselective Lewis acid promoted Diels–Alder reaction and an olefin ring-closing metathesis to close a strained 11-membered macrocycle.

Synthetic Methods

K. Ogata,* Y. Atsuumi, D. Shimada,
S.-i. Fukuzawa* ________ **5896 – 5899**

Nickel-Catalyzed Three-Component Coupling between Aryl Aldehydes, Norbornenes, and Silanes Leading to Indanols through Aromatic C–H Bond Activation of Aryl Aldehydes

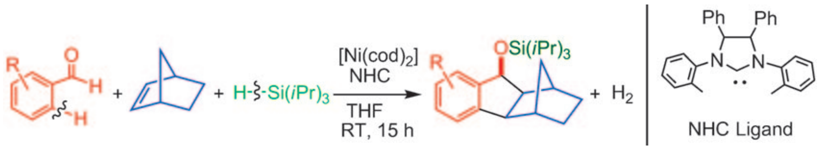

The first example of the title reaction involving the combination of an aryl aldehyde, norbornene, and silane has been developed (see scheme). The reaction involves aromatic C–H bond activation of an aryl aldehyde at the *ortho* position, it proceeded with good diastereoselectively, and is applicable for various aryl aldehydes and norbornenes or norbornadienes. cod = cycloocta-l,5-diene, THF = tetrahydrofuran, NHC = N-heterocyclic carbene.

Zeolites

X. Liu, U. Ravon, A. Tuel* __ **5900 – 5903**

Evidence for F$^-$/SiO$^-$ Anion Exchange in the Framework of As-Synthesized All-Silica Zeolites

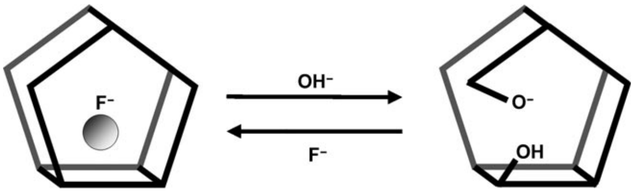

Not everything changes: Charge-compensating anions can be exchanged in as-synthesized zeolite frameworks with changes in both the density of defect sites and of the hydrophobic character of the zeolite. The reversible transformation occurs without dissolution/recrystallization of the zeolite and preserves the size and shape of the crystals (see picture). Fluoride removal is not possible in all-silica D4R units, for which fluoride ions play a structure-directing role.

Li–S Battery

N. Jayaprakash, J. Shen, S. S. Moganty, A. Corona, L. A. Archer* ____ **5904 – 5908**

Porous Hollow Carbon@Sulfur Composites for High-Power Lithium–Sulfur Batteries

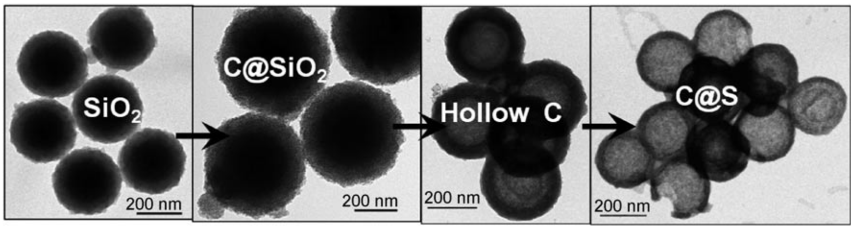

Slowing down the shuttle: C@S nanocomposites (see TEM images) based on mesoporous, hollow carbon capsules were generated by a template-based approach. As the cathode material in a Li–S secondary battery, they display outstanding electrochemical features attributed to sequestration of elemental sulfur in the carbon capsules and to its favorable effect in limiting polysulfide shuttling as well as to enhanced electron transport from the sulfur.

Endofullerenes

L. Feng, Z. Slanina, S. Sato, K. Yoza, T. Tsuchiya, N. Mizorogi, T. Akasaka,* S. Nagase,* N. Martín, D. M. Guldi ____ **5909 – 5912**

Covalently Linked Porphyrin–La@C_{82} Hybrids: Structural Elucidation and Investigation of Intramolecular Interactions

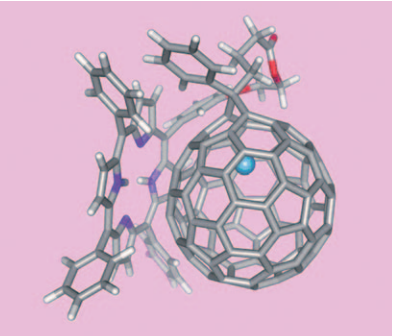

π–π talks: Three isomeric porphyrin–La@C_{82} hybrids were synthesized and structurally characterized for the first time (see picture: La blue sphere, N dark blue, O red). The two chromophores, which have a large π surface, evidently exhibit electronic interactions in the ground state and communicate with each other in the photoexcited state.

Extraction Methods

Q. Liu, J. B. Shi, J. T. Sun, T. Wang, L. X. Zeng, G. B. Jiang* ____ **5913 – 5917**

Graphene and Graphene Oxide Sheets Supported on Silica as Versatile and High-Performance Adsorbents for Solid-Phase Extraction

On the GO: Graphene (G) and graphene oxide (GO) supported on silica are demonstrated to be excellent adsorbents for reversed-phase and normal-phase solid-phase extraction (RP- and NP-SPE) towards various analytes ranging from small molecules to proteins and peptides. Notably, G-bound silica is capable of extracting proteins with large molecular weight and phosphorylated peptides, making it particularly suitable for MALDI-TOF mass spectrometry.

C–H Activation

S. Fan, F. Chen, X. Zhang* _ **5918 – 5923**

Direct Palladium-Catalyzed Intermolecular Allylation of Highly Electron-Deficient Polyfluoroarenes

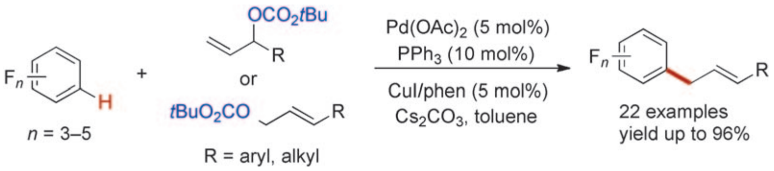

A simple operation: The use of readily available PPh_3, high reaction efficiency, and good stereo- and regioselectivity provided useful and operationally simple access to polyfluoroarylated derivatives through the title transformation (see scheme; phen = 1,10-phenanthroline). The reaction mechanism was also studied.

Cyclic Amines

I. Dubovyk, D. Pichugin,
A. K. Yudin* ———— **5924 – 5926**

Palladium-Catalyzed Ring-Contraction and Ring-Expansion Reactions of Cyclic Allyl Amines

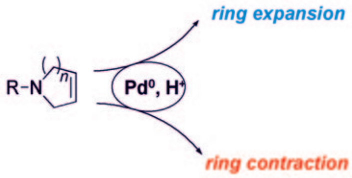

Ring around the rosy: An amino group can act as the leaving group or the nucleophile in a palladium-catalyzed allylic amination. As a result, readily accessible cyclic amines can be either ring contracted or ring expanded (see scheme).

Synthetic Methods

Y.-F. Wang, K. K. Toh, J.-Y. Lee,
S. Chiba* ———— **5927 – 5931**

Synthesis of Isoquinolines from α-Aryl Vinyl Azides and Internal Alkynes by Rh–Cu Bimetallic Cooperation

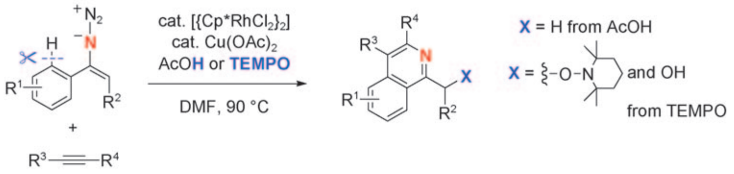

Catalysts in a relay: A synthetic method for delivering highly substituted isoquinolines has been developed (see scheme; Cp* = C_5Me_5, DMF = *N*,*N*-dimethylformamide, TEMPO = 2,2,6,6-tetramethylpiperidine-1-oxyl). A preliminary mechanistic study showed that the rhodium and copper cooperate synergistically in the multistep sequence.

Rhodium Catalysis

F. Miege, C. Meyer,*
J. Cossy* ———— **5932 – 5937**

Rhodium-Catalyzed Cycloisomerization Involving Cyclopropenes: Efficient Stereoselective Synthesis of Medium-Sized Heterocyclic Scaffolds

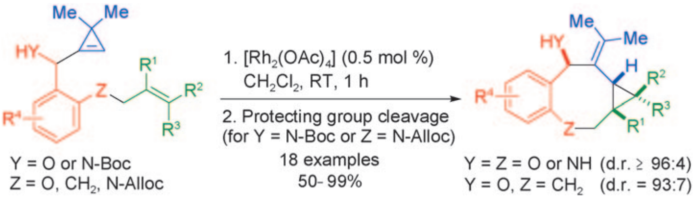

A happy medium: The title reaction of cyclopropenyl carbinols and carbinylamines gives carbo- and heterocycles with a [6.1.0] bicyclic ring fused to an aromatic ring (see scheme, Alloc = allyloxycarbonyl, Boc = *tert*-butyloxycarbonyl). These reactions are the first examples of the formation of medium-sized rings by the intramolecular cyclopropanation of an alkene with a donor-substituted rhodium carbenoid, which is not generated from a diazo compound.

Scaffold Diversity

J. Wu, J. Becerril, Y. Lian, H. M. L. Davies,
J. A. Porco, Jr., J. S. Panek* – **5938 – 5942**

Sequential Transformations to Access Polycyclic Chemotypes: Asymmetric Crotylation and Metal Carbenoid Reactions

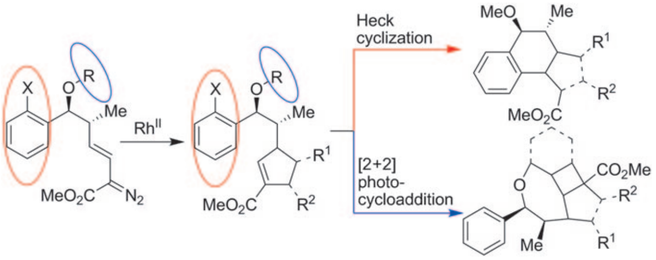

All in order: Bicyclic and tricyclic chemotypes were accessed through the title transformations. By subsequent pairing of installed functional groups using Heck cyclization or [2+2] photocycloaddition, the synthesis of tetracycles, pentacycles, and condensed polycycles has been achieved with high stereochemical and skeletal variation.

Flow Chemistry

T. Noël, S. Kuhn, A. J. Musacchio,
K. F. Jensen,*
S. L. Buchwald* **5943 – 5946**

Suzuki–Miyaura Cross-Coupling Reactions in Flow: Multistep Synthesis Enabled by a Microfluidic Extraction

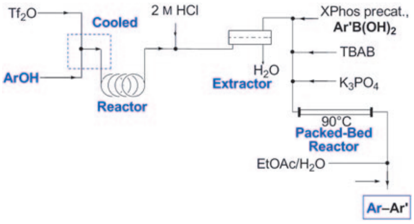

Continuous success: A continuous-flow Suzuki–Miyaura cross-coupling reaction starting from phenols was made possible through use of an efficient microfluidic extraction operation and a packed-bed reactor. Various biaryls were obtained in excellent yield (14 examples). TBAB = $Bu_4N^+Br^-$.

Colloidal Spheres

J. Liu, S. Z. Qiao,* H. Liu, J. Chen, A. Orpe,
D. Y. Zhao, G. Q. Lu* **5947 – 5951**

Extension of The Stöber Method to the Preparation of Monodisperse Resorcinol–Formaldehyde Resin Polymer and Carbon Spheres

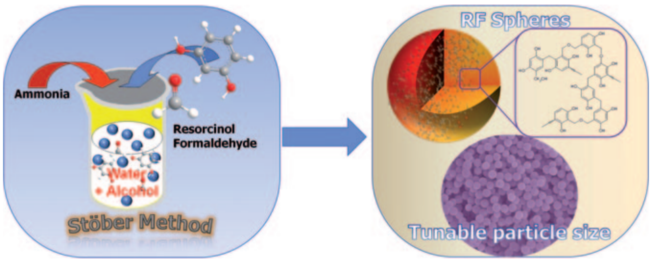

Sphere we go: Monodisperse resorcinol formaldehyde (RF) resin polymer spheres with finely tunable particle size ranging from 200 to 1000 nm (see pictures) are prepared by an extension of the Stöber method. Pyrolysis of the RF spheres at 600 °C under N_2 atmosphere yields uniform carbon spheres with a volume shrinkage of 19 %.

Microreactors

R. A. Maurya, C. P. Park, J. H. Lee,
D.-P. Kim* **5952 – 5955**

Continuous In Situ Generation, Separation, and Reaction of Diazomethane in a Dual-Channel Microreactor

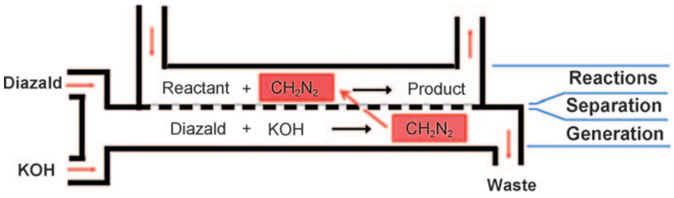

A fierce dog: A method for the continuous in-situ on-demand generation, separation, and reaction of diazomethane in a dual-channel microreactor has been developed (see picture; Diazald = *N*-methyl-*N*-nitroso-*p*-toluenesulfonamide). The microchemical system allows a variety of diazomethane reactions to be performed without the most common problems of preparation, handling, transfer, and decomposition.

Amyloids

A. K. Schütz, A. Soragni, S. Hornemann,
A. Aguzzi, M. Ernst, A. Böckmann,*
B. H. Meier* **5956 – 5960**

The Amyloid–Congo Red Interface at Atomic Resolution

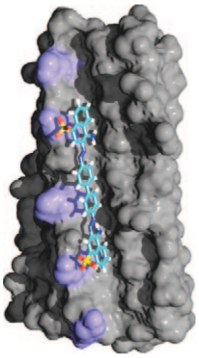

The analytical "gold standard" for amyloid characterization and diagnostics, Congo red, was studied in complex with an amyloid (see picture). Based on details of the binding mode, a point mutation of the amyloid was prepared which has the same three-dimensional structure as the wild-type protein but is not congophilic. This surprising specificity may aid in the design of selective anti-amyloidogenic drugs.

Polyoxometalates

B. S. Bassil, M. Ibrahim, R. Al-Oweini,
M. Asano, Z. Wang, J. van Tol,
N. S. Dalal,* K.-Y. Choi, R. Ngo Biboum,
B. Keita, L. Nadjo, U. Kortz* **5961 – 5964**

A Planar $\{Mn_{19}(OH)_{12}\}^{26+}$ Unit Incorporated in a 60-Tungsto-6-Silicate Polyanion

Manganese in large numbers: The largest number of manganese ions ever incorporated in a polyoxometalate (POM) is found in a planar Mn_{19}-oxo-hydroxo magnetic cluster incorporated in a discrete 60-tungsto-6-silicate (see structure Mn yellow, O red/pink). The compound has interesting structural, magnetic, and electrochemical properties.

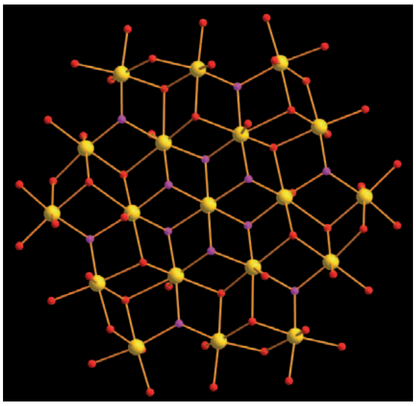

CS_2 Activation

O. P. Lam, F. W. Heinemann,
K. Meyer* **5965 – 5968**

C–C Bond Formation through Reductive Coupling of CS_2 to Yield Uranium Tetrathiooxalate and Ethylenetetrathiolate Complexes

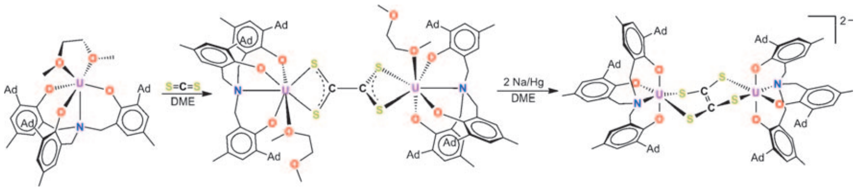

A novel twist: The U^{III} complex $[((^{Ad}ArO)_3N)U]$ reacts with CS_2 by reductive coupling to form the tetrathiooxalate complex $[\{((^{Ad}ArO)_3N)U\}_2(\mu\text{-}\kappa^2{:}\kappa^2\text{-}C_2S_4)]$ with a newly formed C–C bond (see scheme). The U^{IV}/U^{IV} tetrathiooxalate complex features a nonplanar $C_2S_4^{2-}$ unit in an unprecedented $\mu\text{-}\kappa^2{:}\kappa^2$ binding mode. Further reduction gives the ethylenetetrathiolate complex $[Na(dme)_3]_2\text{-}[\{((^{Ad}ArO)_3N)U\}_2(\mu\text{-}C_2S_4)]$. DME = 1,2-dimethoxyethane.

Supporting information is available on www.angewandte.org (see article for access details).

A video clip is available as Supporting Information on www.angewandte.org (see article for access details).

This article is available online free of charge (Open Access).

Service